

## Probabilistic evaluation of liquefaction-induced settlement mapping through multiscale random field models

Qiushi Chen<sup>1</sup>, Chaofeng<sup>2</sup> Wang, Zhe Luo<sup>3</sup> and C. Hsein Juang<sup>4</sup>

<sup>1</sup>Assistant Professor, Glenn Department of Civil Engineering, Clemson University, Clemson, SC 29634 USA. Email: qiushi@clemson.edu

<sup>2</sup>Graduate student, Glenn Department of Civil Engineering, Clemson University, Clemson, SC 29634 USA. Email: chaofew@clemson.edu

<sup>3</sup>Assistant Professor, Department of Civil Engineering, The University of Akron, Akron, OH 44325 USA. Email: zluo@uakron.edu

<sup>4</sup>Glenn Professor, Glenn Department of Civil Engineering, Clemson University, Clemson, SC 29634 USA. Email: hsein@clemson.edu

**Abstract:** Understanding and assessing the spatial extent of liquefaction hazard requires the spatial dependence of geotechnical properties to be taken into account. In this work, novel multiscale random field models will be developed to characterize and quantify spatial variability of geotechnical parameters across scales. Such models will then be integrated with a simplified procedure for the probabilistic evaluation of liquefaction-induced settlements based on in-situ field tests such as the cone penetration test (CPT). Joint distribution of peak ground acceleration and moment magnitude of earthquake will be derived from the Seismic Hazard Maps using a simplified procedure. A unique feature of the proposed work is its ability to refine and obtain higher resolution random fields for geotechnical properties in critical areas, such as adjacent to important infrastructure, or in areas with detailed small-scale field data. The proposed framework is then applied to evaluate the liquefaction-induced settlement of an earthquake-prone area to demonstrate its applicability.

**Keywords:** Liquefaction, multiscale random field, spatial variability, probabilistic analysis.

### 1. Introduction

Assessment of regional liquefaction hazard requires an accurate predictive tool for evaluating not only the probability of liquefaction occurrence, but more importantly, the associated effects within a region. To this end, excessive and differential settlements due to soil liquefaction have been the major causes for infrastructure damages during an earthquake. Evaluation of liquefaction-induced settlement can be expressed in terms of the probability of exceeding a given settlement threshold for seismic hazards within a region for a period of time (e.g., the probability of exceeding 10cm settlement for earthquakes in a 50 year period). Such probabilistic evaluation necessitates the integration of different solution models accounting for: (i) the liquefaction-resistance of a given soil profile; (ii) the spatial dependence of soil properties across scales within the region; (iii) the uncertainty nature of future earthquake

events. This work presents a comprehensive framework integrating those three key ingredients and applies the developed framework to probabilistically assess the liquefaction-induced settlements within an earthquake-prone region.

### 2. General Framework

In this work, empirical models from geotechnical earthquake engineering (e.g., CPT-based liquefaction models) are used in combination with novel geostatistics tools (e.g., multiscale random field models) and seismic hazard models (e.g., joint distribution of peak ground acceleration and moment magnitude) to assess the liquefaction potential over the region of interest.

### 3. The Juang 2013 Procedure for Probabilistic Settlement Exceedance Estimate

To assess the probability of settlement exceeding a given threshold (e.g., 10cm) at a particular location during a given earthquake,

herein, we adopt the procedure proposed by Juang et al. (2013). Key components are discussed in this section.

### 3.1 The Updated Robertson & Wride 1998 model

The Juang 2013 procedure requires the liquefaction potential based on CPT data, herein, we adopt the classical procedure proposed by Robertson and Wride (1998).

The liquefaction potential is evaluated by the factor of safety:

$$FS = \frac{CRR}{CSR} \quad (1)$$

where CRR is the cyclic resistance ratio and CSR is the cyclic stress ratio.

The CRR can be calculated following the Robertson and Wride (1998) procedure as

$$CRR = \begin{cases} 0.833[(q_{c1N})_{cs} / 1000] + 0.05 & \text{if } (q_{c1N})_{cs} < 50 \\ 93[(q_{c1N})_{cs} / 1000]^3 + 0.08 & \text{if } 50 \leq (q_{c1N})_{cs} < 160 \end{cases} \quad (2)$$

where  $(q_{c1N})_{cs}$  is the clean sand equivalent tip resistance.

The CSR is calculated based recommendation in Youd et al. (2001)

$$CSR = 0.65 \left( \frac{a_{max}}{g} \right) \left( \frac{\sigma_{vo}}{\sigma'_{vo}} \right) (r_d) \left( \frac{1}{MSF} \right) \left( \frac{1}{K_\sigma} \right) \quad (3)$$

where  $a_{max}$  = peak horizontal acceleration at the ground surface;  $g$  = acceleration of gravity;  $\sigma_{vo}$ ,  $\sigma'_{vo}$  = total and effective vertical stresses, respectively;  $r_d$  = the shear-stress reduction coefficient; MSF = magnitude scaling factor; and  $K_\sigma$  = overburden correction factor.

### 3.2 Joint distribution of $a_{max}$ and $M_w$

The procedure to obtain joint distribution of  $a_{max}$  and moment magnitude  $M_w$  is adopted from Juang et al. (2008). It consists of three steps:

1. Obtain the joint probability of  $a_{max}$ ,  $M_w$ , and  $PGA > h$  (where PGA is the rock outcrop peak ground acceleration,  $h$  is a specified PGA level) based on the definition of conditional probability as follows:

$$p(a_{max}, M_w, PGA > h) = p[a_{max} | (M_w, PGA > h)] \cdot p(M_w | PGA > h) \cdot p(PGA > h) \quad (4)$$

2. Obtain the joint probability of  $a_{max}$ ,  $M_w$ , and  $h$  (any given PGA level).

$$p(a_{max}, M_w, h) = p[a_{max}, M_w, PGA > h] - p[a_{max}, M_w, PGA > h + \Delta PGA] \quad (5)$$

3. Determine the joint probability mass function of  $a_{max}$  and  $M_w$ .

$$p(a_{max}, M_w) = \sum_h^p p(a_{max}, M_w, h) \quad (6)$$

### 3.3 Maximum likelihood-based volumetric settlement estimation

Following the procedure described previously, the joint probability distribution of  $a_{max}$  and  $M_w$  can be established for a given exposure time of, say, 50 years for a particular location. This joint probability distribution is discretized into a set of 130,000 pairs of  $(a_{max}, M_w)$ , each with corresponding joint probability. For each given pair of  $a_{max}$  and  $M_w$ , the conditional probability of exceeding a particular threshold settlement value, e.g., 10cm, is calculated using the simplified method proposed by Juang et al. (2013).

## 4. Characterization of Spatial Dependence

### 4.1 Spatial correlation

In this study, spatial correlation is described using a form of covariance known as the semivariogram,  $\gamma(\mathbf{h})$ , which is equal to half the variance of the difference of two random variables separated by distance  $\mathbf{h}$

$$\gamma(\mathbf{h}) = \frac{1}{2} \text{Var}[Z(\mathbf{u}) - Z(\mathbf{u} + \mathbf{h})] \quad (6)$$

where  $Z(\mathbf{u})$  is a Gaussian random variable at location  $\mathbf{u}$ . The distance vector  $\mathbf{h}$  can be expressed as

$$\mathbf{h} = \sqrt{\left( \frac{h_1}{a} \right)^2 + \left( \frac{h_2}{b} \right)^2} \quad (7)$$

where  $h_1$  and  $h_2$  are the centroidal separation distance along the field's major and minor axes, respectively, corresponding to the vector distance  $\mathbf{h}$ . Scalar quantities 'a' and 'b' specify how quickly spatial dependence decreases along those axes and are related to the correlation length. The correlation between two samples separated by distance  $\mathbf{h}$  is related to the value of semivariogram

$$\rho(\mathbf{h}) = 1 - \gamma(\mathbf{h}) \quad (8)$$

#### 4.2 Sequential simulation process

Given the probability distribution of a parameter value at single location and their spatial dependence specified by the semivariogram, a sequential simulation approach is implemented, which consists of simulating each value individually, conditional upon all previously simulated values (Chen et al. 2012, Chen et al. 2015). The distribution of the next point to be simulated, denoted as  $Z_n$ , conditional upon all previous simulated data, denoted as  $\mathbf{Z}_p$ , is given by a univariate normal distribution with updated mean and variance

$$(Z_n | \mathbf{Z}_p) \sim N(\Sigma_{np} \cdot \Sigma_{pp}^{-1} \cdot \mathbf{z}_p, \sigma_n^2 - \Sigma_{np} \cdot \Sigma_{pp}^{-1} \cdot \Sigma_{pn}) \quad (9)$$

$\sigma_n^2$  = covariance of the next simulated point; and  $\Sigma_{np}, \Sigma_{pn}, \Sigma_{pp}$  = covariance matrices. Details of the simulation process can be found in Chen et al. 2015.

#### 4.3 Multiscale extension

In this study, the previously described procedure to characterize soil spatial variability is extended to incorporate multiple scales of resolution. As an example, we consider two scales of interest, i.e., scale ‘1’ for coarse scale and scale ‘2’ for fine scale. The coarse scale is defined as the average of all fine-scale points within its area (element). Correlations between all considered scales can be calculated by expanding the definition of covariance

$$\rho_{Z_{1(a)}, Z_{1(b)}} = \frac{\sum_{i=1}^N \sum_{j=1}^N \rho_{Z_{2i(a)}, Z_{2j(b)}}}{\sqrt{\sum_{i=1}^N \sum_{j=1}^N \rho_{Z_{2i(a)}, Z_{2j(a)}}} \sqrt{\sum_{i=1}^N \sum_{j=1}^N \rho_{Z_{2i(b)}, Z_{2j(b)}}}} \quad (10)$$

$$\rho_{Z_2, Z_{1(a)}} = \frac{\sum_{i=1}^N \rho_{Z_{2i(a)}, Z_{2i(a)}}}{\sqrt{\sum_{i=1}^N \sum_{j=1}^N \rho_{Z_{2i(a)}, Z_{2j(a)}}}} \quad (11)$$

where  $\rho_{Z_{1(a)}, Z_{1(b)}}$  is the correlation between two coarse scale (scale ‘1’) elements ‘a’ and ‘b’;

$\rho_{Z_2, Z_{1(a)}}$  is the correlation between a fine scale element (scale ‘2’) and coarse element ‘a’.

### 5. Illustrative Examples

The proposed framework is illustrated by applying to an example region – the west part of the Alameda County, California, USA, which provides a comprehensive case history of seismic effects at a specific site.

#### 5.1 Analysis region

The USGS has conducted extensive post-earthquake investigation in Alameda County following the 1989 Loma Prieta earthquake (Bennett 1990). The moist unit weight of soil above water table and the saturated unit weight of soil are adopted as  $\gamma_m = 15.0 \text{ kN/m}^3$  and  $\gamma_{sat} = 19.4 \text{ kN/m}^3$ . The CPT data used in this paper are collected from USGS website (<http://earthquake.usgs.gov/research/cpt/data/alameda/>). The water table information is available in CPT data. Locations of all the 211 CPT soundings and the outline of the studied region are shown in Fig. 1.

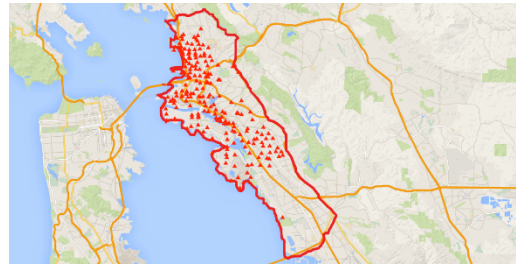


Figure 1. Map of the Alameda County and 211 CPT sounding locations

#### 5.2 Probabilistic settlement exceedance at individual sounding locations

The probability of exceeding 10 cm settlement in 50 years (referred as POE in the following) at each CPT location is calculated using the method stated in Section 3. The results are summarized as a histogram shown in Fig. 2, which shows that at most of the CPT locations the probability of exceedance of 10 cm settlement is close to zero.

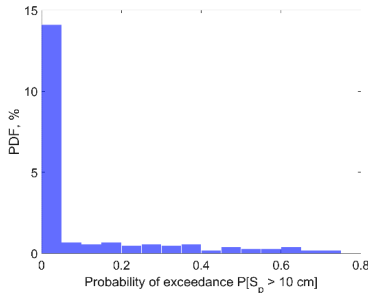


Figure 2. Histogram of the POE at CPT soundings

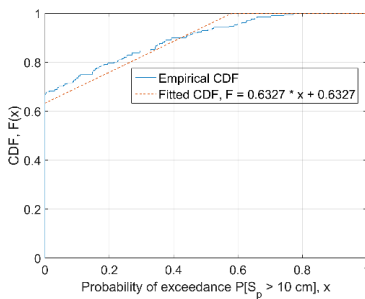


Figure 3. CDF of the POE at CPT soundings

The empirical cumulative density function of the probability of exceedance is also plotted and fitted to a linear function shown in Fig. 3. This will facilitate the multiscale random field simulation in the following section.

### 5.3 Multiscale random field simulations

Given the POE at CPT soundings, the probability of exceedance at other locations will be realized through random field models described in Section 4. A normal score mapping technique has been used in the present study to transform variables between Gaussian distributions and non-Gaussian distributions in order to take advantage of the desirable Gaussian properties in describing spatial correlations (Chen et al. 2012). With the fitted CDF (Fig. 3), the transformation between the two distributions is made possible.

The semivariogram is also calculated and fitted to an exponential curve shown in Fig. 4. The correlation length is found to be 1211 m, hence

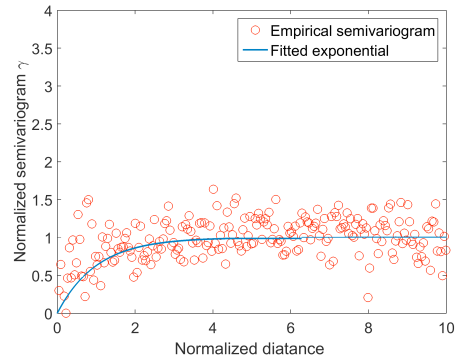


Figure 4. Semivariogram fitting

the spatial correlation against the distance can be expressed as

$$\rho(h) = e^{-\frac{h}{a}} \quad (7)$$

in which  $h$  is the distance between two locations and  $a=1211$  m is the correlation length.

Conditional sequential simulation process described in Section 4 is then used to generate probability values at unknown locations, which depend on the probabilities at the original 211 CPT locations as well as any previously generated data points. A unique and novel aspect of the random field models is the ability to selectively and consistently access and generate small-scale detailed data points in critical areas and/or in areas where soil information is known to greater details (e.g., CPT sounding locations). Monte Carlo simulations of both single and multi-scale random fields are performed.

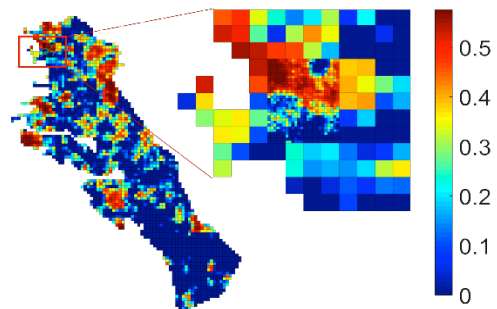


Figure 5(a). Random field of probability obtained from one simulation

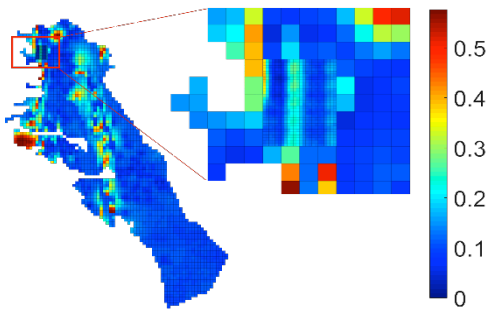


Figure 5(b). Random field of probability obtained from the average of 1,000 simulations

Sample realizations of random fields of probabilities are shown in Fig. 5 with different levels of resolution. In this example, multi-scale random fields have been generated at a selected block as highlighted in Fig. 5. The comparison between single scale random fields with multi-scale random fields shows that the multi-scale random fields show same levels of probabilities as corresponding single scale fields. However, with more information provided by the small-scale random field, there are much higher resolutions in selected critical areas. This is a crucially important point about the proposed methodology, since it essentially provides a consistent way of linking small-scale information with large-scale region liquefaction assessment. It allows one to analyze in great details liquefaction susceptibility at selected locations, while consistently maintaining information at much larger scale. This will be illustrated by analyzing the settlement risk underneath the selected block showing in the next section.

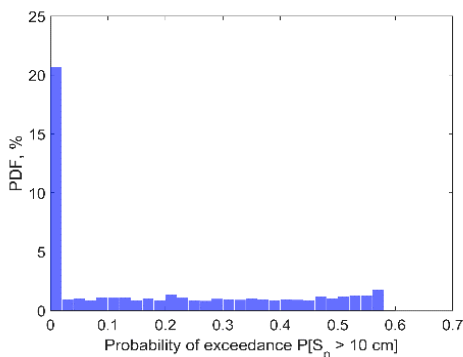


Figure 6. Histogram of probability of exceedance

The histogram of simulated values (Fig. 6) has the same shape with that of the original values (Fig. 4). Results shown in Fig. 6 suggest the desired spatial structure is preserved in the simulations.

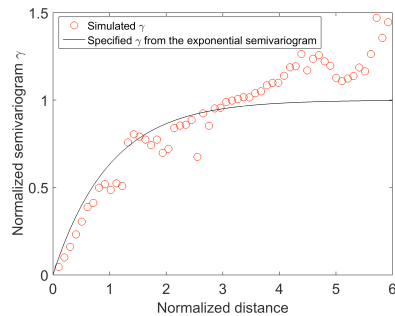


Figure 7. Semivariogram

#### 5.4 Liquefaction-induced settlement assessment

This section shows the probabilistic assessment of liquefaction-induced settlement within the region of interest, based on the results from Monte Carlo simulations. Each Monte Carlo simulation shown in the previous section represents one realization of desired properties (e.g., probability of exceedance) consistent with random field characterizations of the input parameters, which account for the spatial variability of soil properties across scales as well as known field data at selected locations. When a large number of simulations are performed, those illustrations can be summarized to assist settlement assessment. Various quantities of interest can be defined. As an example, we evaluate the cumulative frequency distribution of the POEs following the methodology proposed in Holzer et al. (2006).

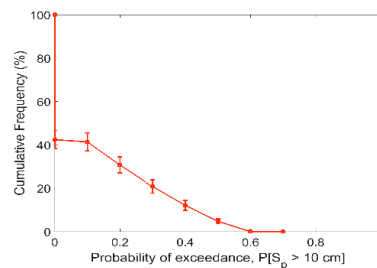


Figure 8. Cumulative frequency results from 1,000 simulations

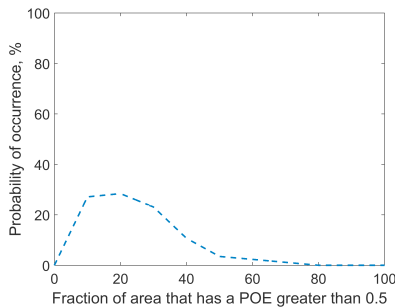


Figure 9. Probability of occurrence versus fraction of the area under the selected block that has a POE greater than 0.5

Figure 8 shows the cumulative frequency of the probabilities of exceedance, based on the results of a total of 1,000 Monte Carlo simulation. The error bar (one standard deviation) is also included in the cumulative frequency plots. It can be seen that almost 60% of the simulated values are very close to zero. This is consistent with the histograms shown above.

To illustrate the capability of multiscale random field, the fraction of the area under the selected block that has the POE greater than 0.5 is calculated and is plotted against the probability of occurrence in Fig. 9. It shows that this block is likely to have a probability of 30% that about 20% of its area is subjected to a POE greater than 0.5.

## 6. Conclusions

This paper presents an integrated framework to assess the probability of exceeding a limiting value of liquefaction-induced settlement over a region of interest for a given period of time. The joint distribution of  $a_{max}$  and  $M_w$  is explicitly taken into account. Multiscale random field model is developed to account for spatial structure of quantities of interest and is used to map the probability of exceedance from CPT locations to the whole region. The spatial correlation structure is validated by the calculated semivariogram. Multiscale random field allows one to evaluate local liquefaction hazard consistent with the large scale characterization of spatial structure.

## References

- Bennett, M. 1990. Ground deformation and liquefaction of soil in the Marina district. Effects of the Loma Prieta earthquake on the Marina district, San Francisco, California; Open file rep. 90-253. Denver, Colo: Dept of the Interior. *US Geological Survey*: 44-79.
- Chen, Q., Seifried, A., Andrade, J. E. and Baker, J. W. 2012. Characterization of random fields and their impact on the mechanics of geosystems at multiple scales. *International Journal for Numerical and Analytical Methods in Geomechanics* 36(2): 140-165.
- Chen, Q., Wang, C. and Hsein Juang, C. 2015. CPT-Based Evaluation of Liquefaction Potential Accounting for Soil Spatial Variability at Multiple Scales. *Journal of Geotechnical and Geoenvironmental Engineering*: 04015077.
- Holzer, T. L., Luke Blair, J., Noce, T. E. and Bennett, M. J. 2006. Predicted liquefaction of East Bay fills during a repeat of the 1906 San Francisco earthquake. *Earthquake Spectra* 22(S2): 261-277.
- Juang, C. H., Ching, J., Wang, L., Khoshnevisan, S. and Ku, C.-S. 2013. Simplified procedure for estimation of liquefaction-induced settlement and site-specific probabilistic settlement exceedance curve using cone penetration test (CPT). *Canadian Geotechnical Journal* 50(10): 1055-1066.
- Juang, C. H., Li, D. K., Fang, S. Y., Liu, Z. and Khor, E. H. 2008. Simplified procedure for developing joint distribution of a max and  $M_w$  for probabilistic liquefaction hazard analysis. *J. of Geotech. and Geoenviron. Eng.* 134(8): 1050-1058.
- Robertson, P. and Wride, C. 1998. Evaluating cyclic liquefaction potential using the cone penetration test. *Canadian Geotechnical Journal* 35(3): 442-459.
- Youd, T. L., Idriss, I. M., Andrus, R. D., ..., & Ishihara, K. 2001. Liquefaction resistance of soils: summary report from the 1996 NCEER and 1998 NCEER/NSF workshops on evaluation of liquefaction resistance of soils. *J. of Geotech. and Geoenviron. Eng.*, 127(10), 817-833.